

Supplementary Information

Direct Synthesis of Pure Single-Crystalline Magnéli Phase Ti₈O₁₅ Nanowires as Conductive Carbon-Free Material for Electrocatalysis

Chunyong He,^{1†} Shiyong Chang,^{1,2†} Xiangdong Huang,^{2,*} Qingquan Wang,² Ao Mei²
and Pei Kang Shen^{1,*}

¹ *State Key Laboratory of Optoelectronic Materials and Technologies, School of Physics and Engineering, Sun Yat-sen University, Guangzhou, 510275, PR China.*

² *Automotive Engineering Institute, Guangzhou Automobile Group Co., Ltd, Guangzhou, 510640, PR China.*

[†]These authors contributed equally to this work.

* e-mail: stsspk@mail.sysu.edu.cn; huangxd@gaei.cn.

Schematic diagram of apparatus

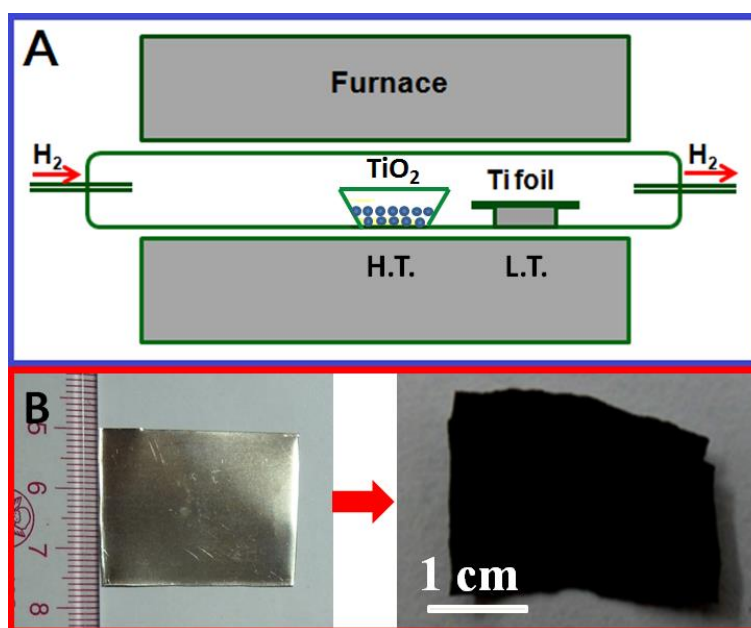
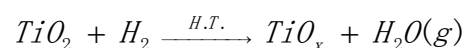


Figure S1 (A) Schematic diagram of the experimental apparatus for growth of Ti_8O_{15} NWs, the temperature decreases gradually from centre to the right, giving two temperature regions: high (H.T.) and low temperature (L.T.), (B) Digital pictures of Ti substrate before and after experiment.

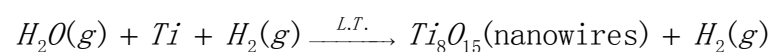
Since no catalyst was used in the process of the growth of the Ti_8O_{15} NWs, suggesting that the growth mechanism of the $\text{KTi}_8\text{O}_{16}$ NWs may not be dominated by the vapor-liquid-solid (VLS) mechanism, which is frequently employed to explain the growth of nanowires and nanoarchitectures.^{S1,S2} Instead, we propose a possible growth mechanism for the formation of the $\text{KTi}_8\text{O}_{16}$ NWs based on the modified vapor-solid (VS) mechanism.^{S3,S4} A two-step path reaction process was proposed in our synthesis process of $\text{KTi}_8\text{O}_{16}$ NWs, showing as follows:

(a) The TiO_2 powders in the quartz boat at the center of the tube (the high temperature

region, H.T.) were reduced to form $H_2O(g)$:



(b) The $H_2O(g)$ reacted with the Ti on the Ti substrate (the low temperature region, L.T.) to form oxygen-deficient tetragonal phase of KTi_8O_{16} NWs in H_2 atmosphere.



Additional experimental data

Calculation Details

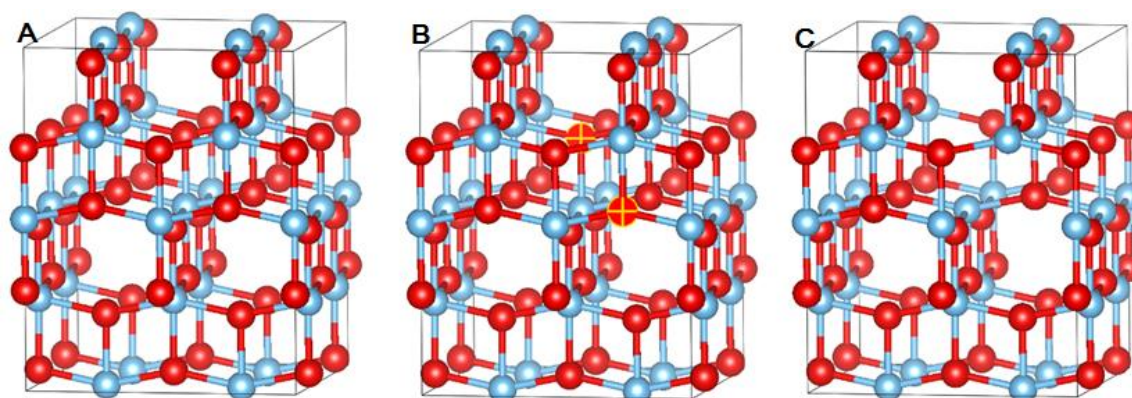


Figure S2 Supercell models of (A) anatase TiO_2 , (B) the site of oxygen vacancy, (C) Magneli phase Ti_8O_{15} .

Anatase TiO_2 has a tetragonal structure with lattice parameters $a = b = 3.776 \text{ \AA}$, $c = 9.486 \text{ \AA}$. To calculate anatase TiO_2 , a $2 \times 2 \times 1$ supercell was constructed with 16 Ti and 32 O atoms, as shown in Figure 1(A). The calculate model of Ti_8O_{15} was constructed from removed two O atoms from anatase TiO_2 supercell and optimized the atomic structure, as shown in Figures 1(B)–1(C).

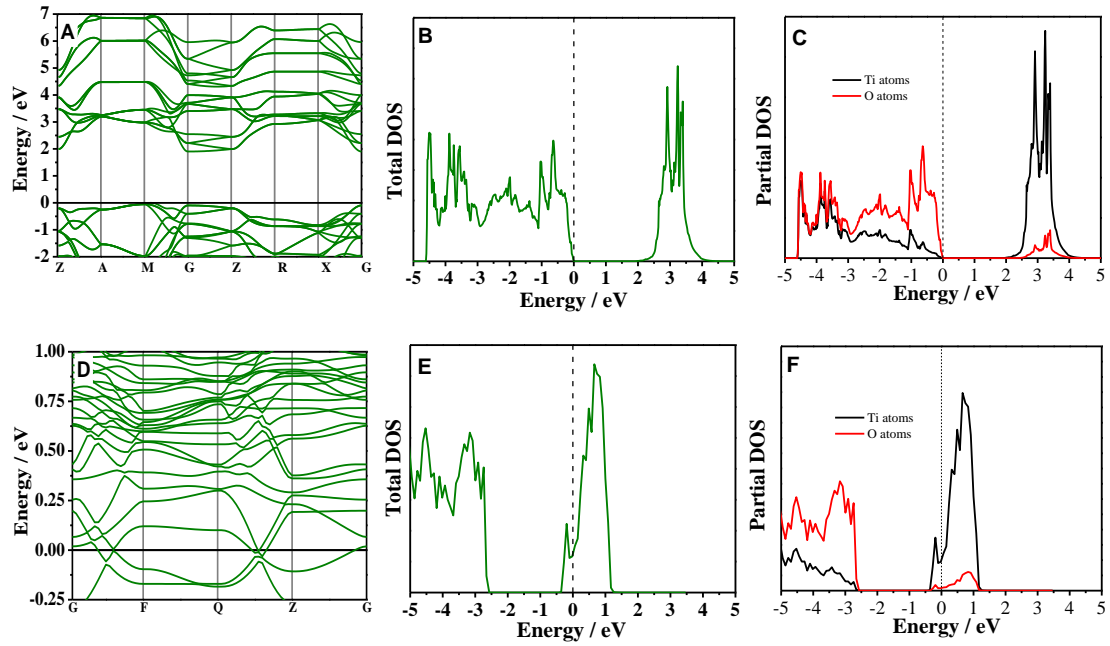


Figure S3 Energy-band diagram, total density of states and partial density of states of anatase TiO₂(A,B,C) and Magneli phase Ti₈O₁₅(D,E,F).

First-principles calculations were performed using the CASTEP module in Materials Studio 5.0 developed by Accelrys Software Inc. Electron-ion interactions were modeled using ultrasoft pseudopotentials in the Vanderbilt form. The states Ti: $3s^2 3p^6 3d^2 4s^2$ and O: $2s^2 2p^4$ were treated as valence states. The wave functions of the valence electrons were expanded through a plane wave basis-set and the cut off energy was selected as 500 eV. The Monkhorst-Pack scheme Kpoints grid sampling was set at $7 \times 7 \times 7$ in the supercells. The convergence threshold for self-consistent iterations was set at 5×10^{-7} eV. The lattice parameters and atomic positions for each supercell system were first optimized using the generalized gradient approximation (GGA) together with the method. The optimization parameters were set as follows: energy change = 5×10^{-6} eV/atom, maximum force = 0.01 eV/Å, maximum stress = 0.02 GPa, and maximum displacement tolerance = 0.005 Å.

The electronic structure of magneli phase titanium suboxide Ti_8O_{15} are studied by using the plane-wave ultrasoft pseudopotential method based on the density functional theory. The band structure reveals that the energy band gap of Ti_8O_{15} is reduced a lot compared with that of anatase TiO_2 , which is due to the fact that $\text{O}2\text{p}$, $\text{Ti}3\text{p}$ and $\text{Ti}3\text{d}$ of Ti_8O_{15} shift toward the left compared with those of TiO_2 , and a new electron energy level formed by the redundant electrons of $\text{Ti}3\text{d}$ and $\text{Ti}3\text{p}$ of Ti_8O_{15} due to the lack of oxygen atom in lattice. The results from density of states (DOS) analysis show that electron distribution near the Fermi level of Ti_8O_{15} is different from that of anatase TiO_2 , contribution of $\text{O}2\text{p}$ to Fermi level decrease and that of $\text{Ti}3\text{d}$ increase, compared with anatase TiO_2 which only has high electrical conductivity, because its narrow forbidden band width results in the Transitions of Electron from the valence band to the conduction band energy required to reduce.

Conductivity Measurements

To measure the conductivity under conditions of low energy and bias voltages, a voltage ramp of 0–0.05 V was applied across split electrodes in steps of 0.025 V for two-probe measurements using a source meter (Keithley 2400). For each measurement, after allowing the exponential decay of the transient ionic current, the steady-state electronic current for each voltage was measured every second over a minimum period of 100 s using a Labview data acquisition program (National Instruments). The time-averaged current for each applied voltage was calculated to create the current–voltage (I–V) characteristics. For the two-probe measurement, the

linearity of the I–V characteristics was maintained by applying an appropriate low voltage/current. The dissipative power was kept under 1×10^{-6} W to eliminate self-heating effects.

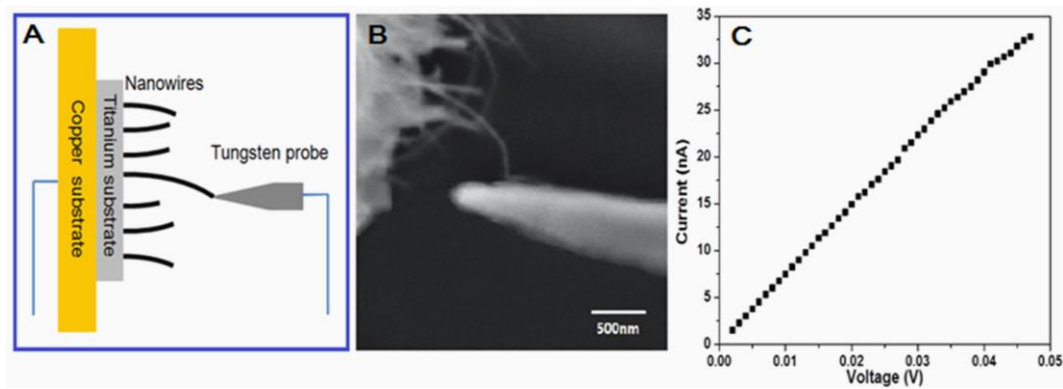


Figure S4. (A) Schematic diagram of the conductivity measuring experiment, (B) SEM image of Ti_8O_{15} nanowire electrode, (C) I–V characteristics of a single Ti_8O_{15} nanowire at room temperature.

Microscopic morphological characteristics

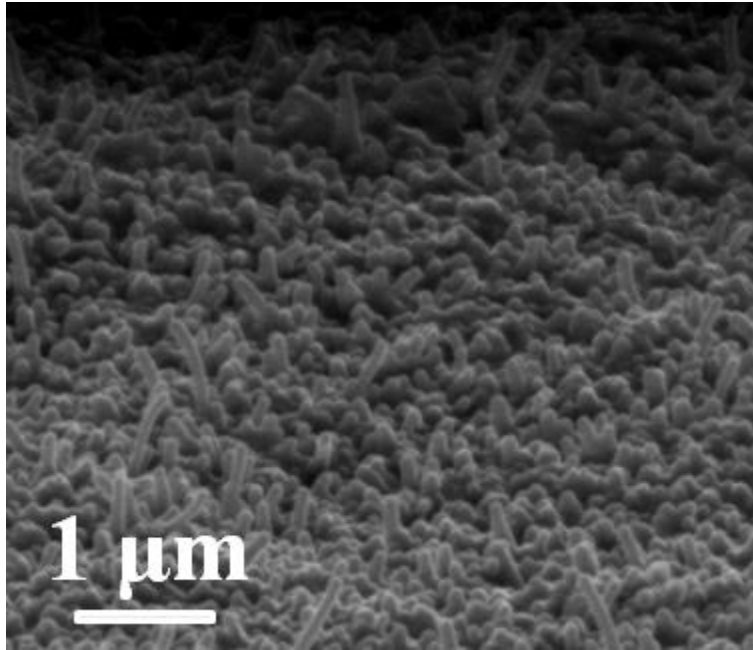


Figure S5. SEM image of club-shaped Ti_8O_{15} nanoparticles, which were formed in the initial stage of the growth of Ti_8O_{15} NWs.

Electrochemical performance

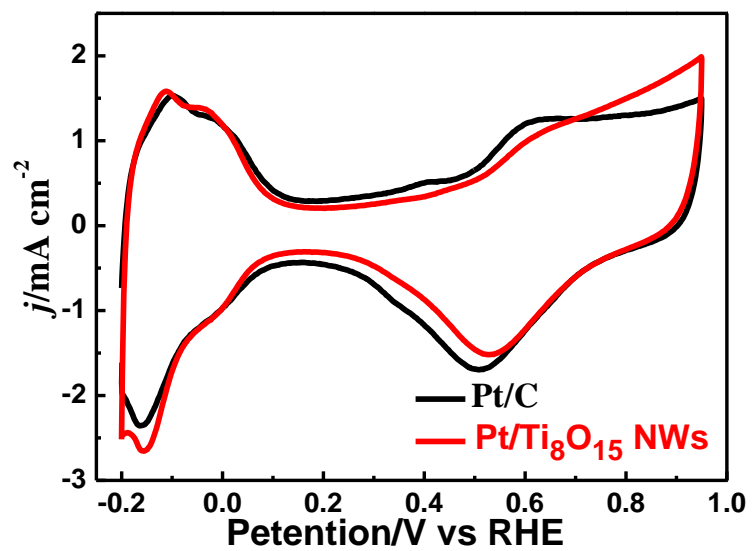


Figure S6. Cyclic voltammograms of Pt/C and Pt/Ti₈O₁₅ NWs in 0.5 mol L⁻¹ H₂SO₄ with the scan rate of 20 mV s⁻¹ at 30 °C

Microscopic morphological characteristics

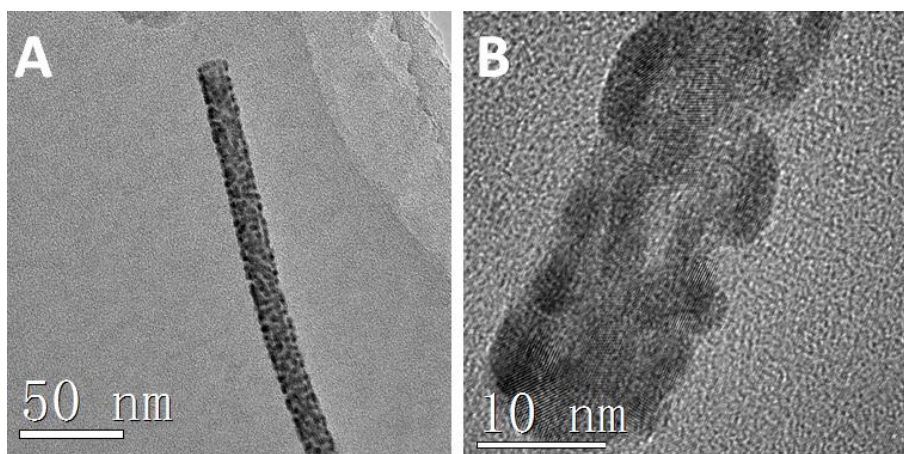


Figure S6. (A,B) TEM images of Pt/Ti₈O₁₅ NWs after 6,000 cycles.

References

- S1 Y. Hao, G. Meng, Z. L. Wang, C. Ye, L. Zhang, *Nano Lett.* 2006, **6**, 1650-1655.
- S2 X. Duan, C. M. Lieber, *Adv. Mater.* 2000, **12**, 298-302.
- S3 J. Zhou, N. S. Xu, S. Z. Deng, J. Chen, J. C. She, Z. L. Wang, *Adv. Mater.* 2003, **15**, 1835-1840.
- S4 Z. W. Pan, Z. R. Dai, Z. L. Wang, *Science* 2001, **291**, 1947-1949.